

Supplementary Info

Ni(II) Complexes of the Phosphine-Oxime Ph₂PC₆H₄-2-CH=NOH

Debashis Basu, Toby J. Woods, Thomas B. Rauchfuss*

School of Chemical Sciences

University of Illinois

Urbana, IL 61801, USA

Figure S1. ³¹P-NMR spectrum of [Ni(PCH=NOH)₂](BF₄)₂ (**[1]**)H₂(BF₄)₂ in CD₂Cl₂

Figure S2. ³¹P-NMR spectrum of Ni(PCH=NO)₂ **[1]**⁰ in CD₂Cl₂

Figure S3. ³¹P-NMR spectra of Ni(PCH=NOH)₂Cl₂ **[1]**H₂Cl₂ in selected solvents

Figure S4. ¹⁹F-NMR spectrum of [Ni(PCH=NO)₂BF₂]BF₄ (**[(1)BF₂]BF₄**) in CH₂Cl₂

Figure S5. ESI-MS of [Ni(PCH=NO)₂BF₂]BF₄ (**[(1)BF₂]BF₄**) in CH₂Cl₂ in positive mode

Figure S6. ³¹P-NMR spectrum of [Ni(PCH=NO)₂BF₂]BF₄ (**[(1)BF₂]BF₄**) in CH₂Cl₂

Figure S7. Cyclic voltammogram of [Ni(PCH=NO)₂BF₂]BF₄ (**[(1)BF₂]BF₄**) in CH₂Cl₂

Figure S8. ¹⁹F-NMR spectrum of reaction mixture of PCH=NOH/Ni(C₆F₅)₂(THF)₂ (1:1)

Figure S9. ¹⁹F-NMR spectra of [Ni(C₆F₅)(PCH=NO)]₂ (**(2)**) in THF and CD₂Cl₂

Figure S10. ³¹P-NMR spectra of [Ni(C₆F₅)(PCH=NO)]₂ (**(2)**) in THF-d⁸ and CD₂Cl₂

Figure S11. ³¹P-NMR spectrum of [Ni(C₆F₅)(PCH=NO)]₂ (**(2)**) in CD₂Cl₂ under air

Figure S12. ³¹P-NMR spectra of [Ni(PCH=NOH)]Cl₂ **[3]** in various solvents

Figure S13. ³¹P-NMR spectrum: reaction of Ni(PCH=NO)₂ with HBF₄/ H(Et₂O)₂BAR^F₄

Scheme S1. Synthetic scheme of (**[4]BF₄**) from PCH=NOH and [Ni(H₂O)₆](BF₄)₂

Figure S14. ³¹P-NMR spectrum of [Ni₃(PCH=NO)₃O]BF₄ (**[4]BF₄**) in CD₂Cl₂

Scheme S2. Synthetic scheme of (**[5](BF₄)₂**) from PCH=NOH and [Ni(CH₃CN)₆](BF₄)₂

Scheme S3. Hypothesis for making (**[5](BF₄)₂**) from PCH=NOH and [Ni(CH₃CN)₆](BF₄)₂

Figure S15. ³¹P-NMR spectrum of (**[5](BF₄)₂**) in CD₂Cl₂

Crystallographic Details

Figure S1. ^{31}P -NMR spectrum of $[\text{Ni}(\text{PCH}=\text{NOH})_2](\text{BF}_4)_2$ (**1**) H_2 (BF_4) $_2$ in CD_2Cl_2

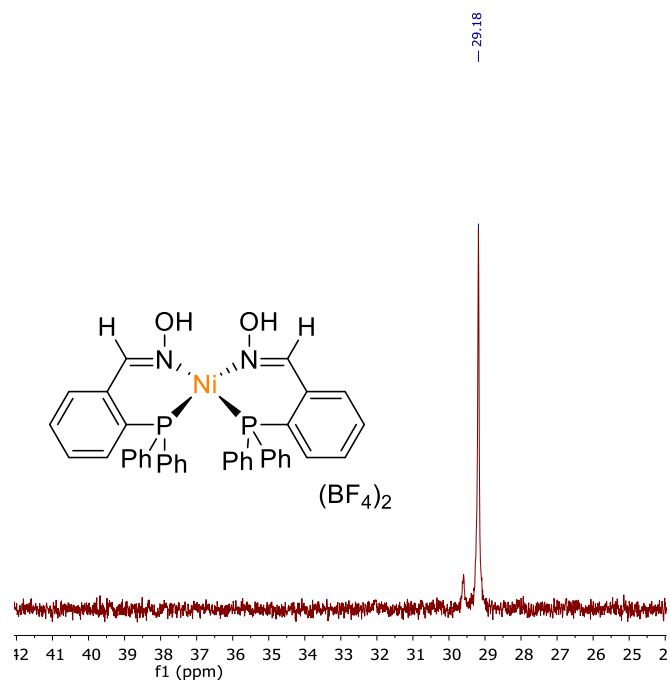


Figure S2. ^{31}P -NMR spectrum of $\text{Ni}(\text{PCH}=\text{NO})_2$ in CD_2Cl_2 .

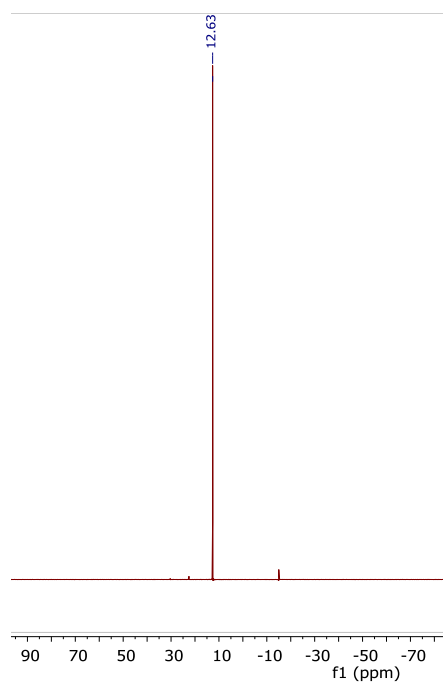


Figure S3. ^{31}P -NMR spectra of $\text{Ni}(\text{PCH}=\text{NOH})_2\text{Cl}_2$ in selected solvents.

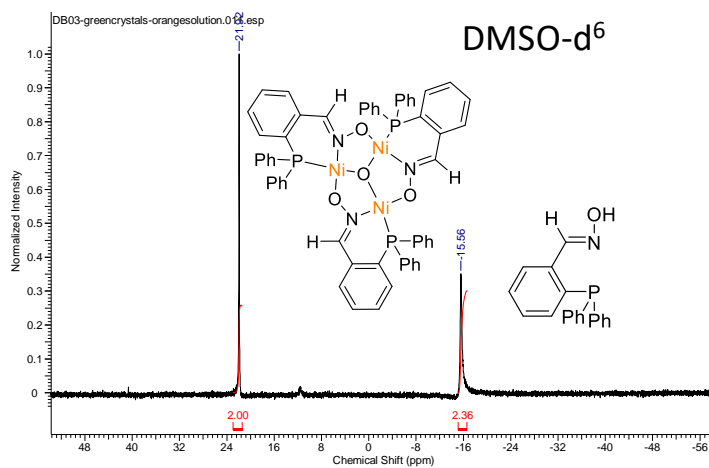
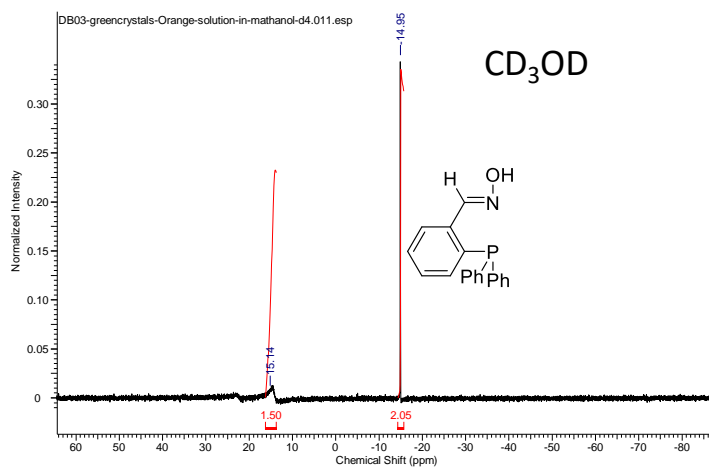


Figure S4. ^{19}F -NMR spectrum of $[\text{Ni}(\text{PCH}=\text{NO})_2\text{BF}_2]\text{BF}_4$ in CH_2Cl_2 .

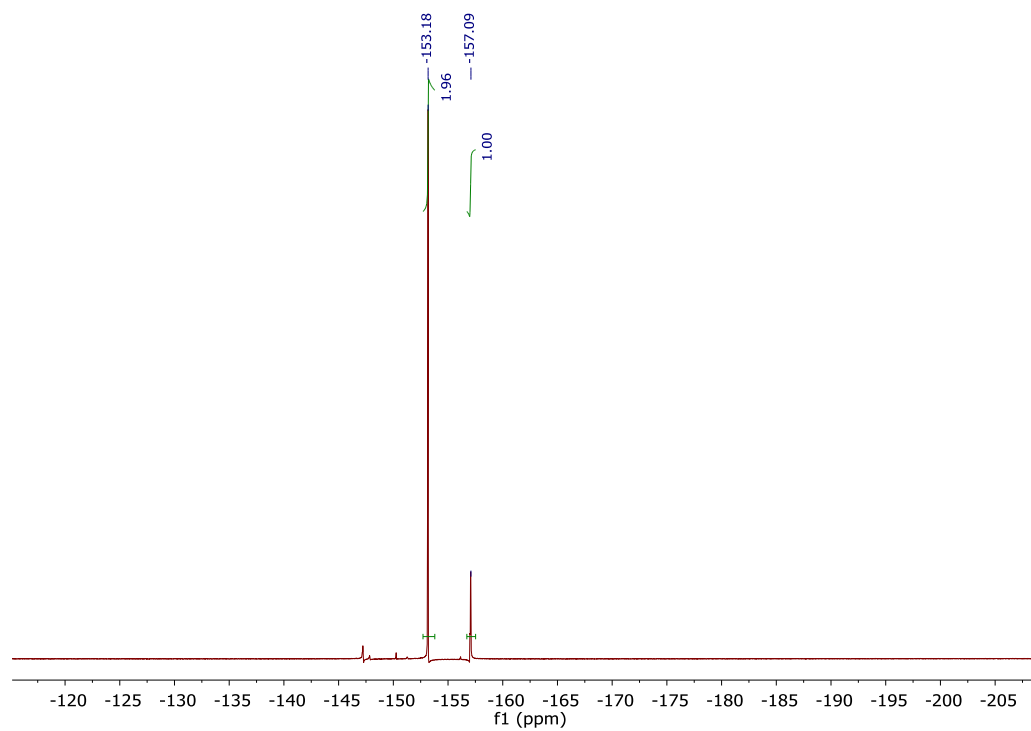


Figure S5. ESI-MS of $[\text{Ni}(\text{PCH}=\text{NO})_2\text{BF}_2]\text{BF}_4$ ($[(1)\text{BF}_2]\text{BF}_4$) in CH_2Cl_2 in positive mode.

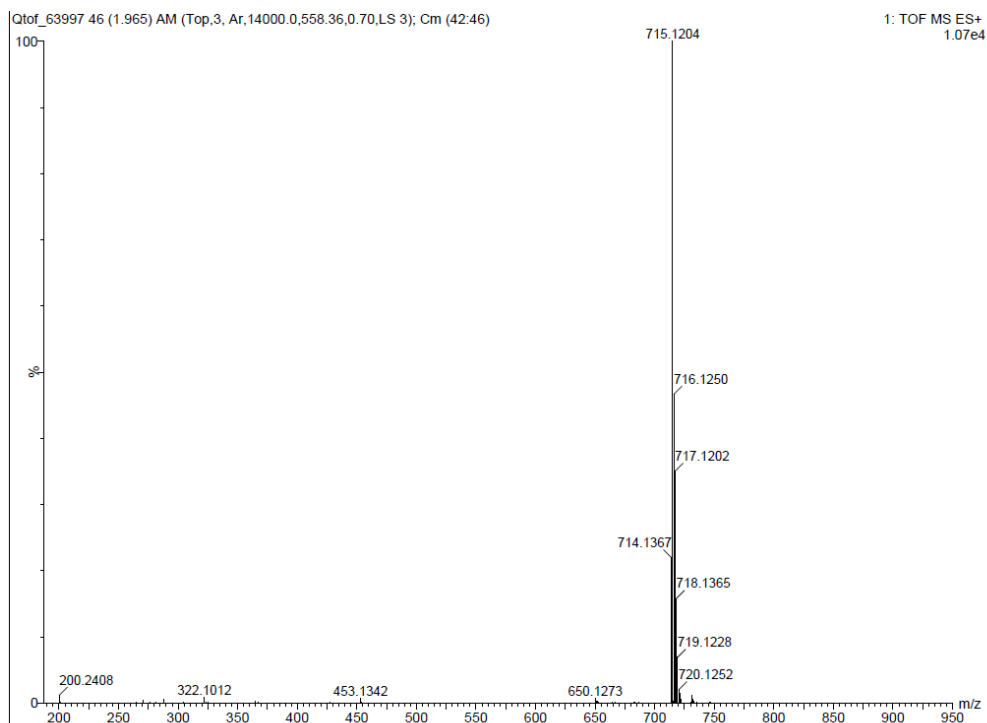


Figure S6. ^{31}P -NMR spectrum of $[\text{Ni}(\text{PCH}=\text{NO})_2\text{BF}_2]\text{BF}_4$ in CH_2Cl_2 .

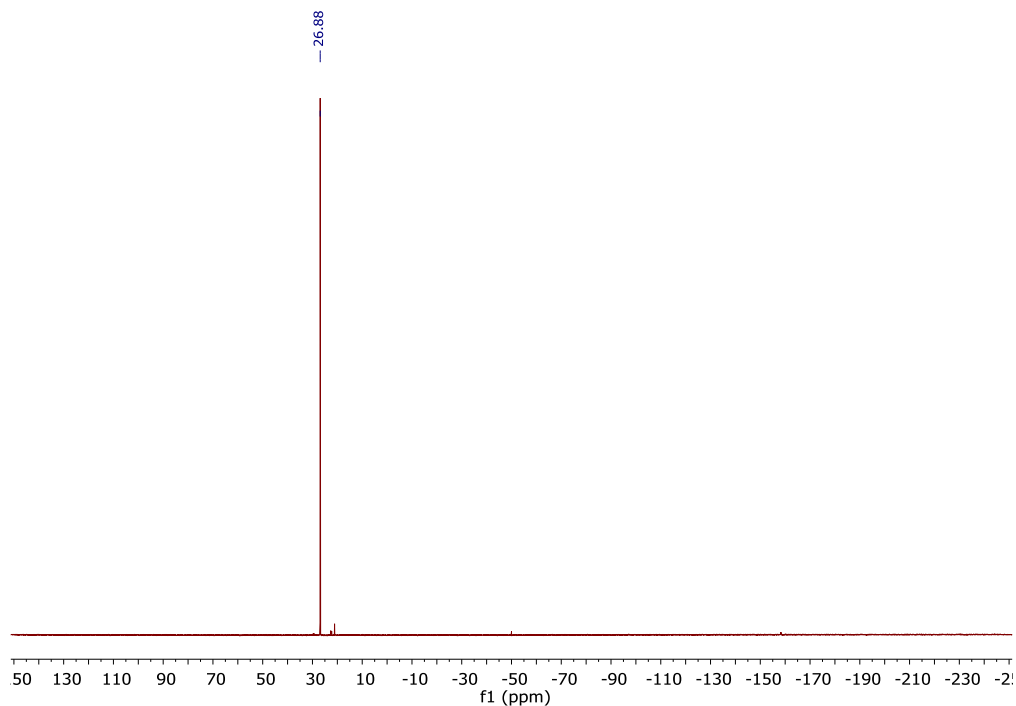


Figure S7. Cyclic voltammogram of $[\text{Ni}(\text{PCH}=\text{NO})_2\text{BF}_2]\text{BF}_4$ ($[\text{(1)BF}_2]\text{BF}_4$) in CH_2Cl_2 with 0.1 M TBAPF₆ as the supporting electrolyte. Electrodes used: Glassy carbon (working); Platinum wire (auxillary); Ag/AgCl (supporting). Scan rate: 100 mV/s vs Fc/Fc⁺. $E_{\text{p,c}}$: -0.96 V; $E_{\text{p,a}}$: -600 V.

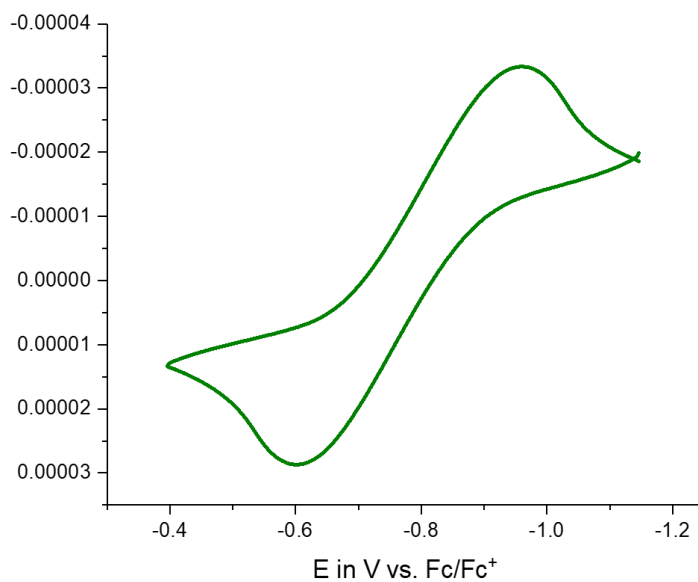


Figure S8. ^{19}F -NMR spectrum of the reaction mixture upon combining PCH=NOH and $\text{Ni}(\text{C}_6\text{F}_5)_2(\text{THF})_2$ (1:1).

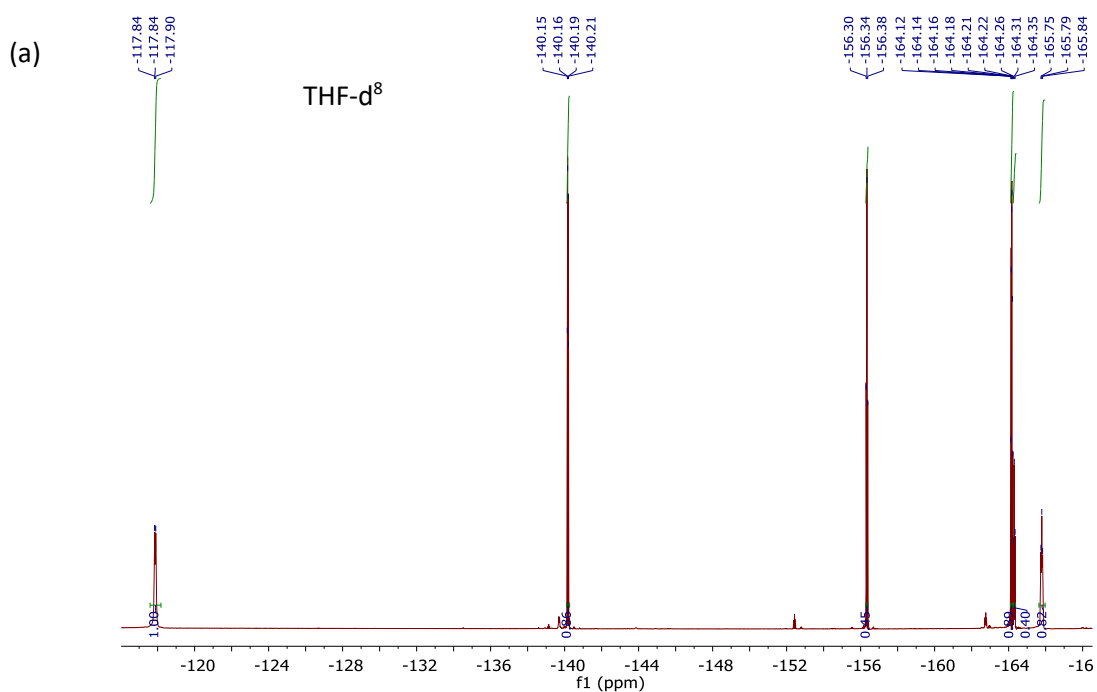
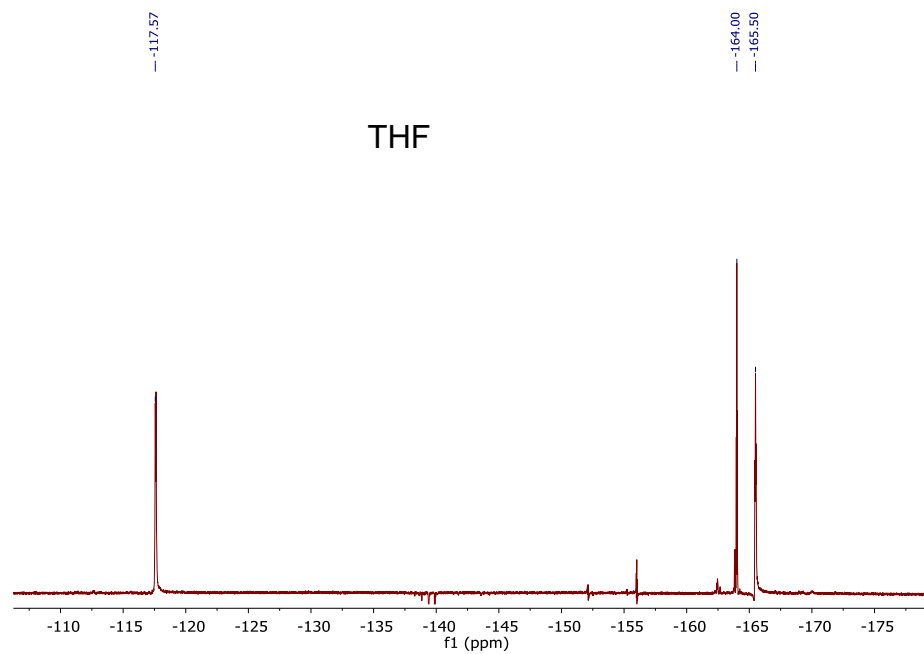


Figure S9. ^{19}F -NMR spectra of $[\text{Ni}(\text{C}_6\text{F}_5)(\text{PCH}=\text{NO})]_2$ in THF and CD_2Cl_2 .



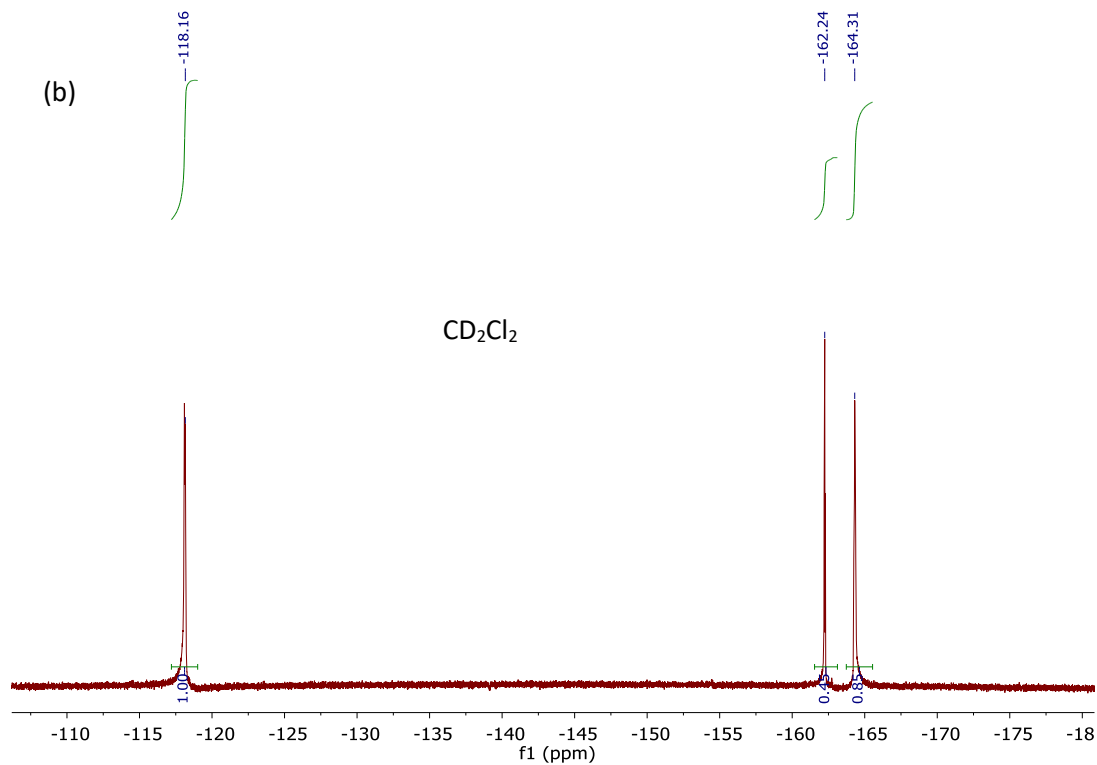
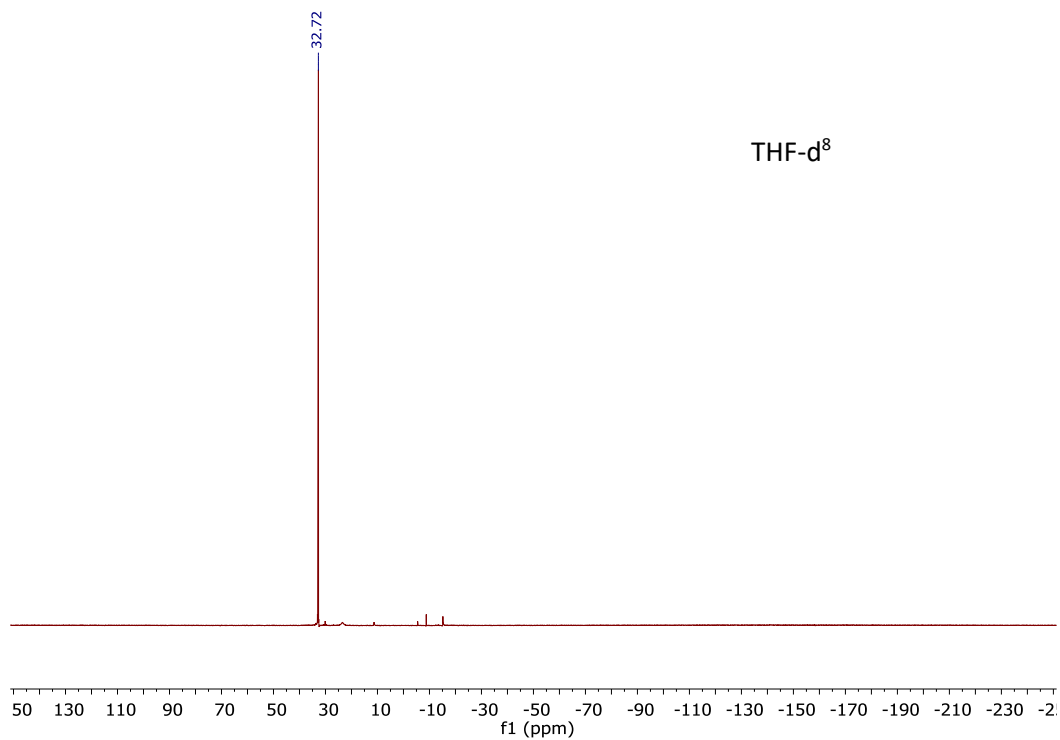


Figure S10. ³¹P-NMR spectra of [Ni(C₆F₅)(PCH=NO)]₂ (**2**) in THF-d⁸ and CD₂Cl₂



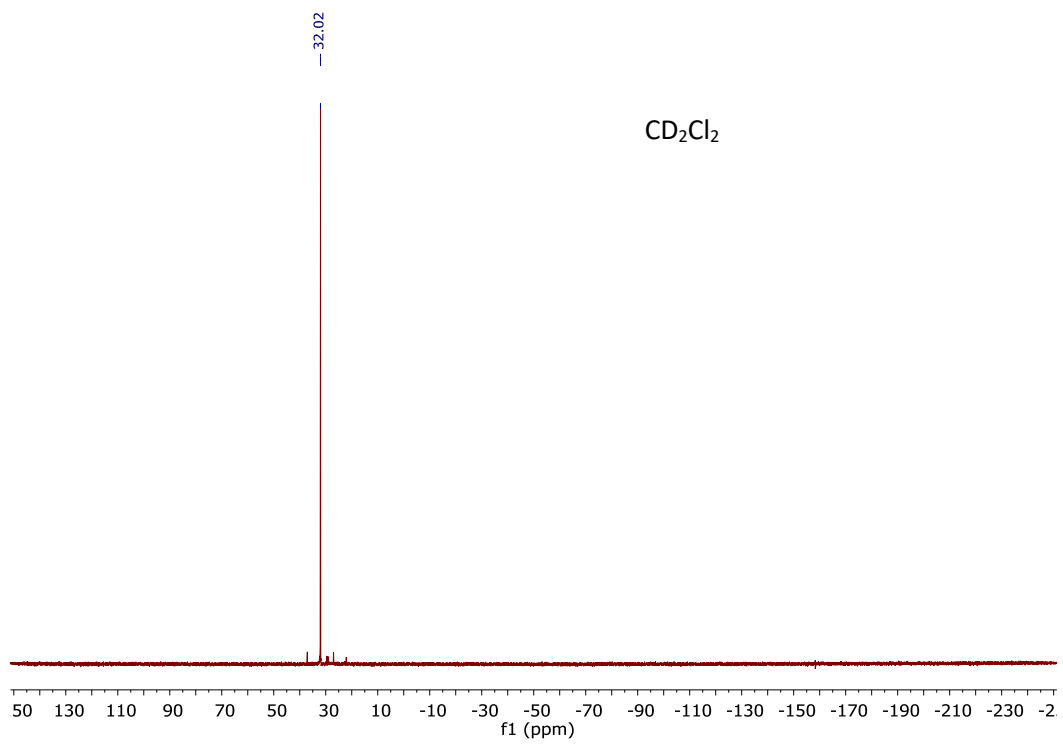


Figure S11. ^{31}P -NMR spectrum of $[\text{Ni}(\text{C}_6\text{F}_5)(\text{PCH}=\text{NO})]_2$ in CD_2Cl_2 under air.

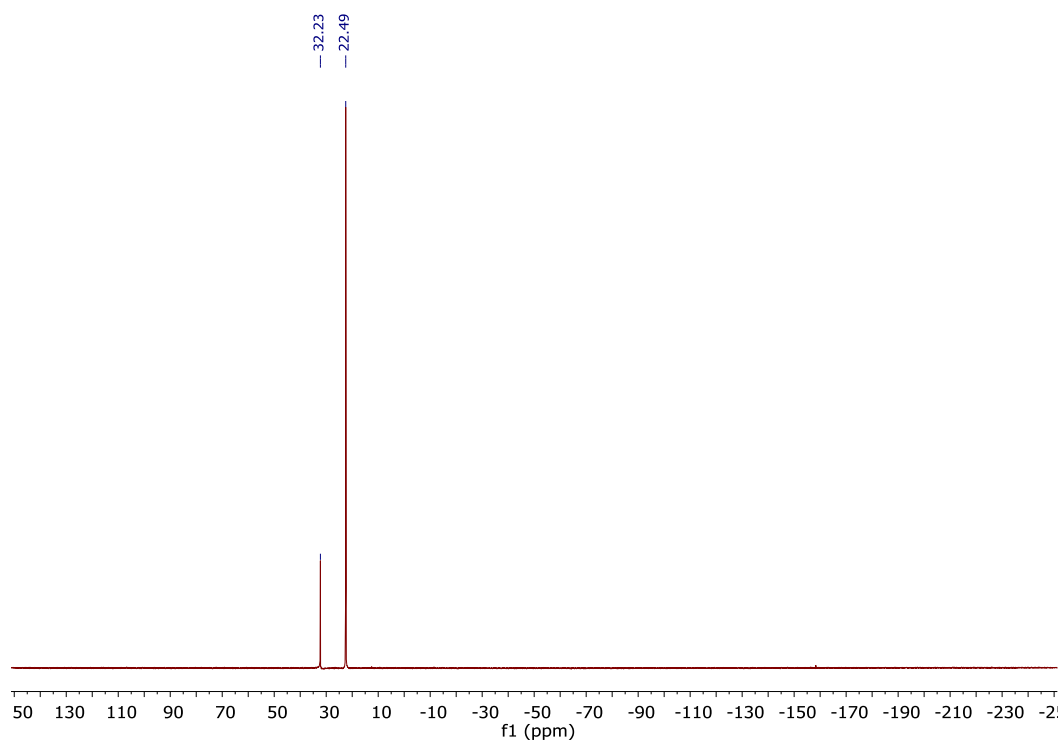


Figure S12. ^{31}P -NMR spectra of $[\text{Ni}(\text{PCH}=\text{NOH})]\text{Cl}_2$ (**3**) in various solvents.

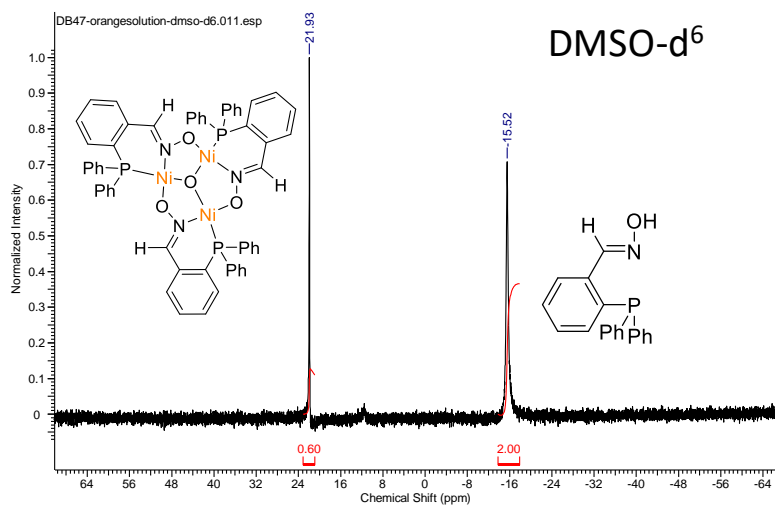
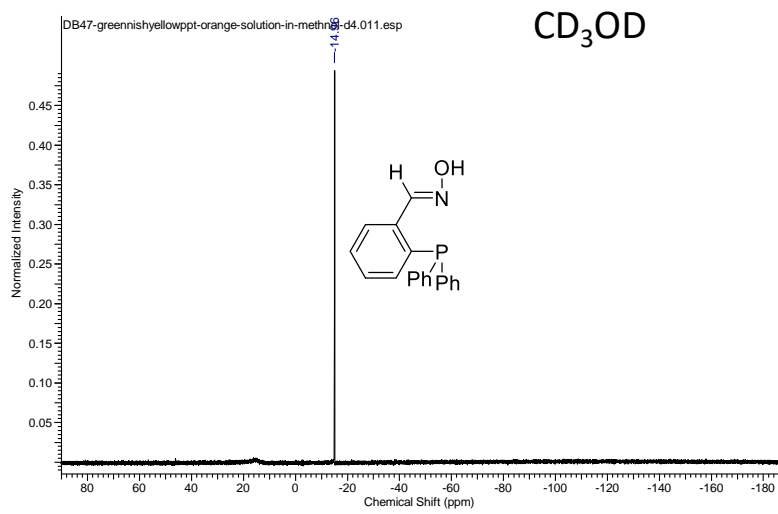
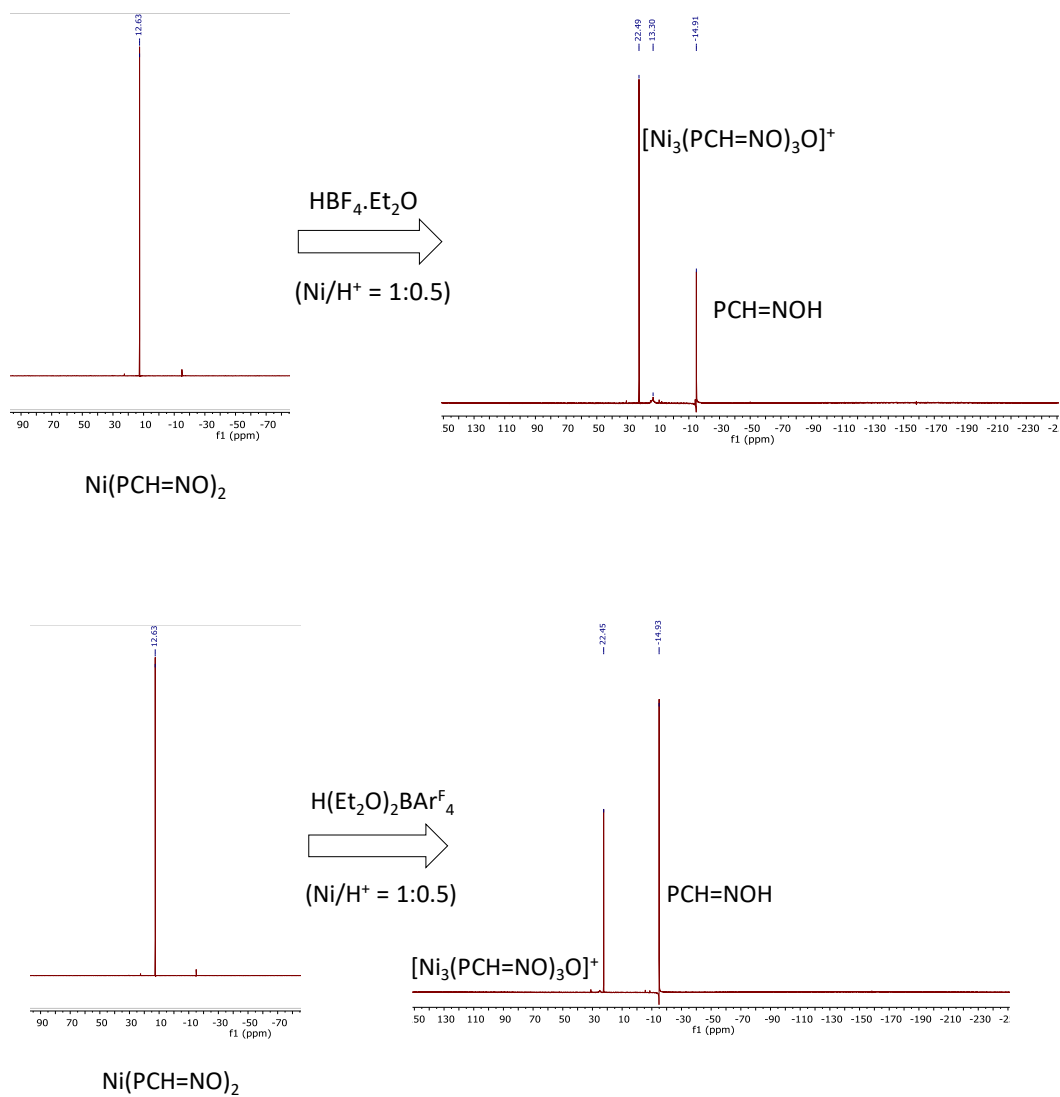


Figure S13. ^{31}P -NMR spectral monitor for the reactions $\text{Ni}(\text{PCH}=\text{NO})_2 + \text{HBF}_4$ and $\text{Ni}(\text{PCH}=\text{NO})_2 + \text{H}(\text{Et}_2\text{O})_2\text{BAr}^{\text{F}}_4$ in CD_2Cl_2 .



Scheme S1. Synthetic scheme of $[\mathbf{4}]\text{BF}_4$ from $\text{PCH}=\text{NOH}$ and $[\text{Ni}(\text{H}_2\text{O})_6](\text{BF}_4)_2$

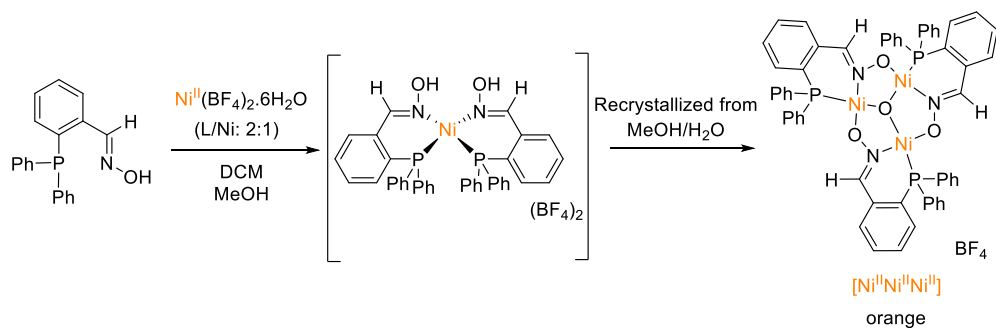
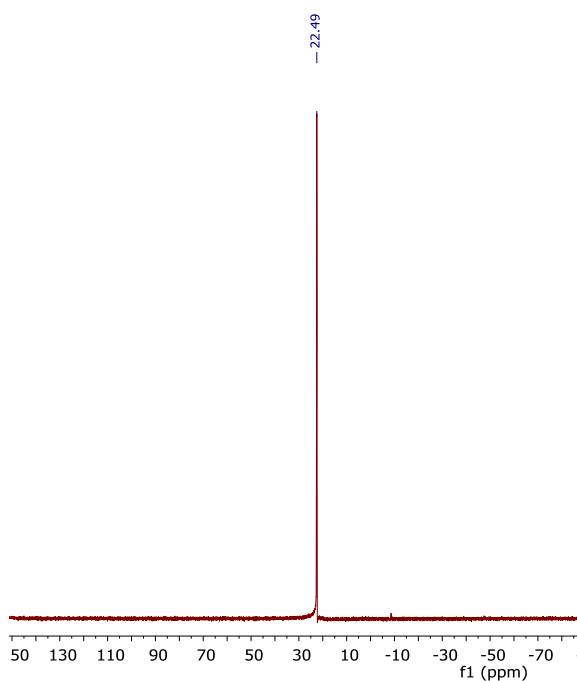
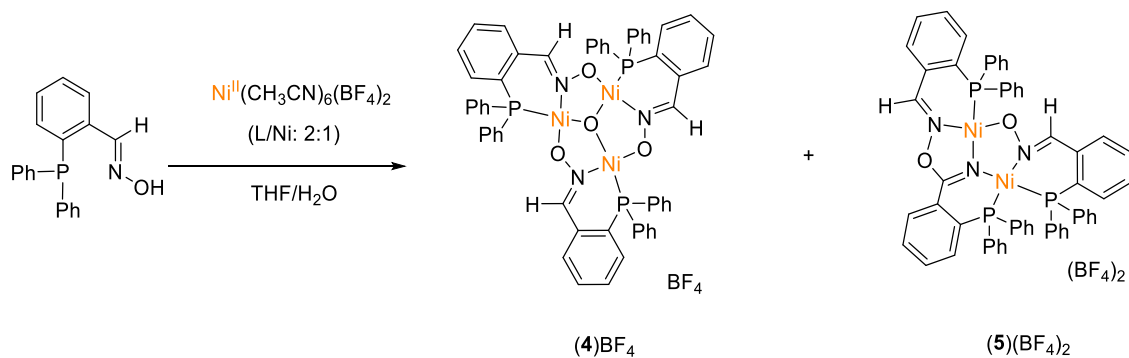


Figure S14. ^{31}P -NMR spectrum of $[\text{Ni}_3(\text{PCH}=\text{NO})_3\text{O}]\text{BF}_4$ in CD_2Cl_2 .



Scheme S2. Synthetic scheme for the reaction of $\text{PCH}=\text{NOH}$ and $[\text{Ni}(\text{CH}_3\text{CN})_6](\text{BF}_4)_2$.



Scheme S3. Hypothesis for formation of $[\mathbf{5}](\text{BF}_4)_2$ from $\text{PCH}=\text{NOH}$ and $[\text{Ni}(\text{CH}_3\text{CN})_6](\text{BF}_4)_2$ ($\text{S} = \text{Solvent}$).

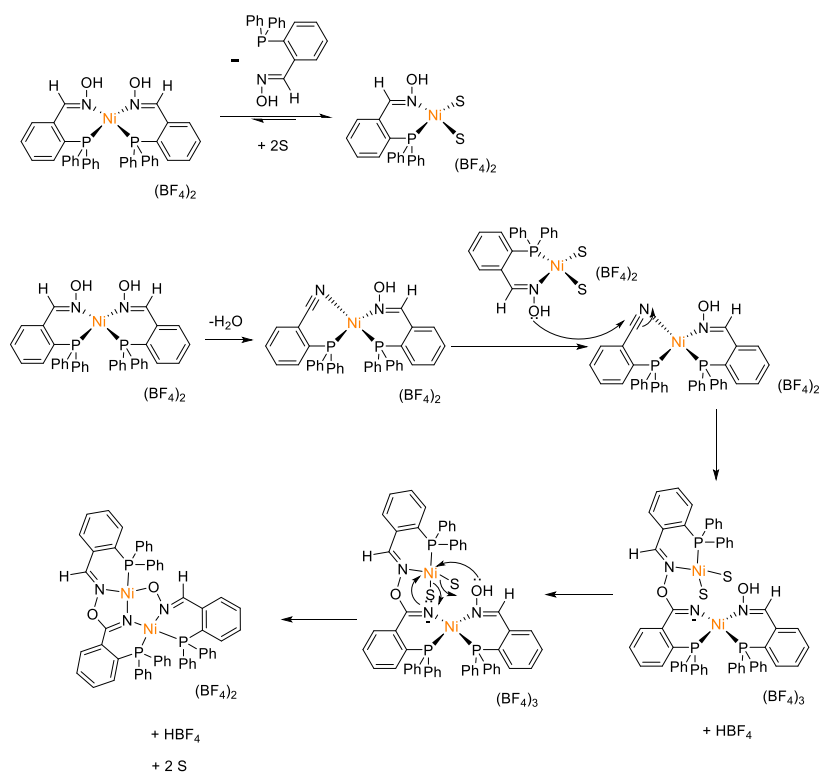
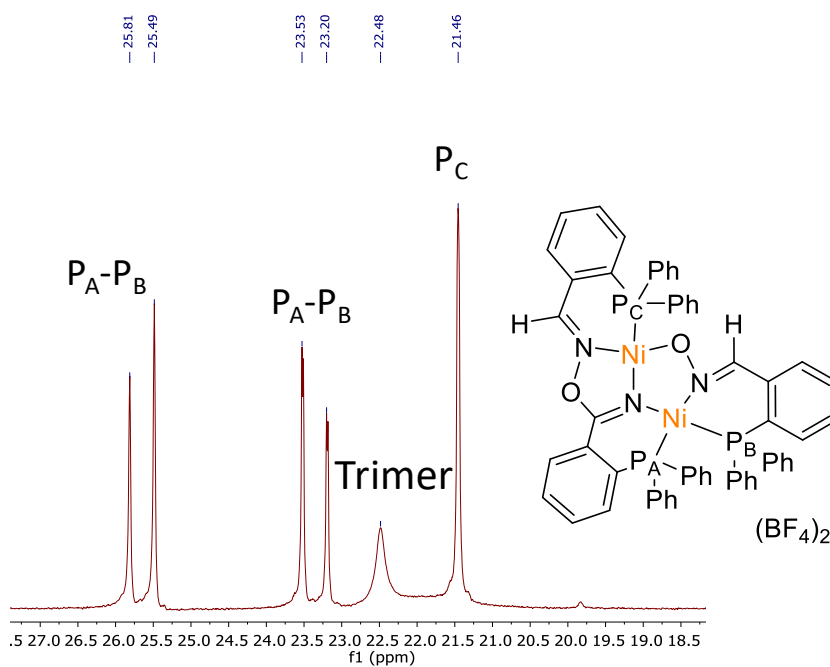
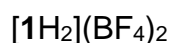


Figure S15. ^{31}P -NMR spectrum of $[\mathbf{5}](\text{BF}_4)_2$ in CD_2Cl_2



Crystallographic Details:



Intensity data were collected on a Bruker D8 Venture kappa diffractometer equipped with a Photon 100 CMOS detector. An I μ s microfocus Mo source ($\lambda = 0.71073 \text{ \AA}$) coupled with a multi-layer mirror monochromator provided the incident beam. The sample was mounted on a 0.3 mm loop with the minimal amount of Paratone-N oil. Data was collected as a series of φ and/or ω scans. Data was collected at 100 K using a cold stream of N_{2(g)}. The collection, cell refinement, and integration of intensity data was carried out with the APEX3 software.¹ A semi-empirical absorption correction was performed with SADABS.² The structure was phased with direct methods using SHELXS³ and refined with the full-matrix least-squares program SHELXL.³

A structural model consisting of one-half of the target molecule plus one tetrafluoroborate counter-anion in the asymmetric unit was developed. Two of the three phenyl rings in the asymmetric unit were found to be disordered over two orientations. For both disordered phenyl rings, similar displacement amplitudes (esd 0.01) were imposed on disordered sites overlapping by less than the sum of van der Waals radii and the P---C bond lengths for each disordered set were restrained to be similar (esd 0.01). All of the disordered phenyl rings were constrained to be perfect hexagons. The site occupancy ratio of the disordered phenyl rings was allowed to freely refine.

The tetrafluoroborate counter-anion was found to be disordered over two orientations. Similar displacement amplitudes (esd 0.01) were imposed on disordered sites overlapping by less than the sum of van der Waals radii. Similarity restraints (esd 0.01) were imposed on like 1,2 and 1,3 distances. The site occupancy ratio of the two orientations was allowed to freely refine.

H atom treatment - The hydroxyl H atom was located in the difference map and its position was allowed to freely refine. At convergence the hydroxyl H atom was in a good hydrogen bonding position.⁴ Remaining H atoms were included as riding idealized contributors. Hydroxyl H atom U's were assigned as 1.5 times U_{eq} of the carrier atom; remaining H atom U's were assigned as 1.2 times carrier U_{eq}.

On the basis of 2152 unmerged Friedel opposites, the fractional contribution of the racemic twin was negligible.^{5,6} The absolute structure parameter y was calculated using PLATON.⁷ The resulting value was $y = 0.002(6)$ indicating that the absolute structure has probably been determined correctly.⁸

The 2 2 0 reflection was omitted from the final refinement due to being partially obscured by the beam stop in some orientations.

[1]⁰

Intensity data were collected on a Bruker D8 Venture kappa diffractometer equipped with a Photon 100 CMOS detector. An I μ s microfocus Mo source ($\lambda = 0.71073 \text{ \AA}$) coupled with a multi-layer mirror monochromator provided the incident beam. The sample was mounted on a 0.3 mm loop with the minimal amount of Paratone-N oil. Data was collected as a series of φ and/or ω scans. Data was collected at 100 K using a cold stream of N_{2(g)}. The collection, cell refinement, and integration of intensity data was carried out with the APEX2 software.⁹ A face-indexed absorption correction was performed numerically with SADABS.² The structure was phased by intrinsic methods using SHELXT¹⁰ and refined with the full-matrix least-squares program SHELXL.³

H atom treatment - All H atoms were included as riding idealized contributors. H atom U's were assigned as 1.2 times carrier U_{eq}.

On the basis of 6162 unmerged Friedel opposites, the structure was determined to be an inversion twin.^{5,6} The twin law (-1 0 0 0 -1 0 0 0 -1) was incorporated into the final refinement; the twin fractions were allowed to freely refine and converged to 0.329(9):0.671(9).

The 0 1 2, 0 1 -2, 0 0 4, and 0 0 -4 reflections were omitted from the final refinement due to being partially obscured by the beam stop.

CCDC: 1834879

1H₂Cl₂

Intensity data were collected on a Bruker D8 Venture kappa diffractometer equipped with a Photon 100 CMOS detector. An I μ s microfocus Mo source ($\lambda = 0.71073 \text{ \AA}$) coupled with a multi-layer mirror monochromator provided the incident beam. The sample was mounted on a 0.3 mm loop with the minimal amount of Paratone-N oil. Data was collected as a series of φ and/or ω scans. Data was collected at 100 K using a cold stream of N_{2(g)}. The collection, cell refinement, and integration of intensity data was carried out with the APEX2 software.⁹ A face-indexed absorption correction was performed numerically with SADABS.² The structure was phased by direct methods using SHELXS³ and refined with the full-matrix least-squares program SHELXL.³

A structural model consisting of the target molecule plus two dichloromethane solvate molecules in the asymmetric unit was developed. For one of the dichloromethane solvate molecules in the asymmetric unit, one of the chlorine atoms and the carbon atom were found to be disordered over two orientations. The displacement amplitudes of the disordered chlorine atoms were constrained to be the same, as were the displacement amplitudes of the disordered carbon atom. All Cl---C bonds of the

disordered molecule were restrained to be the same (esd 0.01). The site occupancy of the disordered atoms was allowed to freely refine.

H atom treatment - Methyl H atom positions, R-CH₃, were optimized by rotation about R-C bonds with idealized C-H, R--H and H--H distances. The hydroxyl H atoms were located in the difference map and refined to good hydrogen bonding positions.⁴ Remaining H atoms were included as riding idealized contributors. Methyl and hydroxyl H atom U's were assigned as 1.5 times U_{eq} of the carrier atom; remaining H atom U's were assigned as 1.2 times carrier U_{eq}.

Five reflections were omitted from the final refinement due to large differences between F_o² and F_c².

CCDC: 1834880

[(1)BF₂]BF₄

Intensity data were collected on a Bruker D8 Venture kappa diffractometer equipped with a Photon 100 CMOS detector. An I μ s microfocus Mo source ($\lambda = 0.71073 \text{ \AA}$) coupled with a multi-layer mirror monochromator provided the incident beam. The sample was mounted on a 0.3 mm loop with the minimal amount of Paratone-N oil. Data was collected as a series of φ and/or ω scans. Data was collected at 100 K using a cold stream of N_{2(g)}. The collection, cell refinement, and integration of intensity data was carried out with the APEX3 software.¹ A semi-empirical absorption correction was performed with SADABS.² The structure was phased by intrinsic methods using SHELXT¹⁰ and refined with the full-matrix least-squares program SHELXL.³

A structural model consisting of the target molecule, one tetrafluoroborate anion, and one dichloromethane solvent molecule position was developed.

The tetrafluoroborate anion was modeled as disordered over two orientations. Similarity restraints were imposed on like B---F distances (esd 0.01 Å) and on like fluorine-fluorine distances (esd 0.02 Å). Similar displacement amplitudes (esd 0.005) were imposed on disordered sites overlapping by less than the sum of van der Waals radii. The displacement parameters of the two boron positions were constrained to be the same. The site occupancy ratio of the two orientations was allowed to freely refine.

H atom treatment - All H atoms were included as riding idealized contributors; H atom U's were assigned as 1.2 times carrier U_{eq}.

The 0 2 1, 1 3 3, 0 2 5, and 3 0 4 reflections were omitted from the final refinement due to being partially obscured by the beam stop in some orientations.

CCDC: 1838219

(2)

Intensity data were collected on a Bruker D8 Venture kappa diffractometer equipped with a Photon 100 CMOS detector. An I μ s microfocus Mo source ($\lambda = 0.71073 \text{ \AA}$) coupled with a multi-layer mirror monochromator provided the incident beam. The sample was mounted on a 0.3 mm loop with the minimal amount of Paratone-N oil. Data was collected as a series of ϕ and/or ω scans. Data was collected at 100 K using a cold stream of N_{2(g)}. The collection, cell refinement, and integration of intensity data was carried out with the APEX3 software.¹ A semi-empirical absorption correction was performed with SADABS.² The structure was phased by direct methods using SHELXS³ and refined with the full-matrix least-squares program SHELXL.³

The asymmetric unit consists of the host plus one disordered dichloromethane solvate molecule and one disordered part occupancy dichloromethane/pentane site. The disordered dichloromethane was modeled as fully occupied with one Cl atom disordered over 2 orientations. The like C-Cl bond distances were restrained to be similar (esd 0.01). The site that is disordered between pentane and dichloromethane was modeled with idealized rigid fragments from a fragment library.¹¹ The total occupancy of this disordered site was constrained to 1/2. Rigid-bond restraints (esd 0.004) were imposed on displacement parameters for all disordered sites and similar displacement amplitudes (esd 0.01) were imposed on disordered sites overlapping by less than the sum of van der Waals radii.

H atom treatment - H atoms were included as riding idealized contributors and their U's were assigned as 1.2 times carrier U_{eq}.

CCDC: 1834875

(3)

Intensity data were collected on a Bruker D8 Venture kappa diffractometer equipped with a Photon 100 CMOS detector. An I μ s microfocus Mo source ($\lambda = 0.71073 \text{ \AA}$) coupled with a multi-layer mirror monochromator provided the incident beam. The sample was mounted on a 0.3 mm loop with the minimal amount of Paratone-N oil. Data was collected as a series of ϕ and/or ω scans. Data was collected at 100 K using a cold stream of N_{2(g)}. The collection, cell refinement, and integration of intensity data was carried out with the APEX3 software.¹ A semi-empirical absorption correction was performed with SADABS.² The structure was phased by intrinsic methods using SHELXT¹⁰ and refined with the full-matrix least-squares program SHELXL.³

H atom treatment - The hydroxyl H atom was located in the difference map, however, attempts to let the H atom position refine led to non-chemically reasonable geometries. As such, the hydroxyl H atom position, R-OH, was optimized by rotation about R-O bonds with idealized O-H and R--H distances. This led to a reasonable H-bonding orientation for the hydroxyl H atom.⁴ Remaining H atoms were included as riding

idealized contributors. Hydroxyl H atom U's were assigned as 1.5 times U_{eq} of the carrier atom; remaining H atom U's were assigned as 1.2 times carrier U_{eq} .

The 1 0 1, -1 0 1, and 1 0 3 reflections were omitted from the final refinement due to being partially obscured by the beam stop in some orientations.

CCDC: 1834878

[4]BF₄

Intensity data were collected on a Bruker D8 Venture kappa diffractometer equipped with a Photon 100 CMOS detector. An I μ s microfocus Mo source ($\lambda = 0.71073 \text{ \AA}$) coupled with a multi-layer mirror monochromator provided the incident beam. The sample was mounted on a 0.3 mm loop with the minimal amount of Paratone-N oil. Data was collected as a series of φ and/or ω scans. Data was collected at 100 K using a cold stream of N_{2(g)}. The collection, cell refinement, and integration of intensity data was carried out with the APEX2 software.⁹ A semi-empirical absorption correction was performed with TWINABS.¹² The structure was phased by intrinsic methods using SHELXT¹⁰ and refined with the full-matrix least-squares program SHELXL.³

A structural model consisting of the target molecule plus one disordered water solvate molecule plus one disordered methanol solvate molecule in the asymmetric unit was developed; however, positions for the idealized methanol solvate molecule were poorly determined, even when considering three separate orientations for the methanol molecule. This model converged with $wR2 = 0.1782$ and $R1 = 0.0614$ for 703 parameters with 4 restraints against 9844 data. Since positions for the solvate molecules were poorly determined a second structural model was refined with contributions from the methanol solvate molecules removed from the diffraction data using the bypass procedure in PLATON.¹³ No positions for the host network differed by more than two su 's between these two refined models. The electron count from the "squeeze" model converged in good agreement with the number of solvate molecules predicted by the complete refinement. The "squeeze" routine identified one void space containing electron density consistent with two methanol molecules, making the most likely solution one with one methanol solvate molecule per target molecule.

The water solvate molecule was found to be disorderd about an inversion center. Residual electron density corresponding to the water hydrogen atoms was visible in the difference Fourier map but the hydrogen positions were unstable when freely refined. For the final refinement the water molecule hydrogen atoms were constrained to an idealized geometry.¹¹

H atom treatment - The remaining non-water H atoms were included as riding idealized contributors. Water H atom U's were assigned as 1.5 times U_{eq} of the carrier atom; remaining H atom U's were assigned as 1.2 times carrier U_{eq} .

All crystals examined exhibited non-merohedral twinning (which consists of a 4° rotation roughly about the a axis). One distinct cell was identified using APEX2⁹ and Cell_Now.¹⁴ Ten frame series were integrated and filtered for statistical outliers using SAINT¹⁵ then corrected for absorption by the multi-scan method using TWINABS¹⁶. Combined unit cell parameters were determined from both components using SAINT.¹⁵ The twin law by rows was (0.994 -0.000 -0.016), (0.028 1.012 0072), (-0.026 -0.078 0.988). Averaged reflections from only the primary orientation were used for phasing and refinement. Refinement against both orientations was attempted but led to higher R factors and less satisfactory placement of the water hydrogen atoms. No decay correction was applied.

CCDC: 1834876

[5](BF₄)₂

Intensity data were collected on a Bruker D8 Venture kappa diffractometer equipped with a Photon 100 CMOS detector. An I μ s microfocus Mo source ($\lambda = 0.71073 \text{ \AA}$) coupled with a multi-layer mirror monochromator provided the incident beam. The sample was mounted on a 0.3 mm loop with the minimal amount of Paratone-N oil. Data was collected as a series of ϕ and/or ω scans. Data was collected at 100 K using a cold stream of N_{2(g)}. The collection, cell refinement, and integration of intensity data was carried out with the APEX3 software.¹ A semi-empirical absorption correction was performed with SADABS.² The structure was phased by intrinsic methods using SHELXT¹⁰ and refined with the full-matrix least-squares program SHELXL.³

A structural model consisting of the target molecule, two tetrafluoroborate anions, plus five dichloromethane solvate molecules in the asymmetric unit was developed.

One of the tetrafluoroborate anions was modeled as disordered over two orientations. All 1,2 and 1,3 distances of the disordered components were restrained to be similar to those of the ordered tetrafluoroborate anion (esd 0.02 \AA). Similar displacement amplitudes (esd 0.01) were imposed on disordered sites overlapping by less than the sum of van der Waals radii. The site occupancy ratio of the two orientations was allowed to freely refine.

One of the dichloromethane solvate molecules was modeled as disordered over two orientations. Similarity restraints (esd 0.01 \AA) were imposed on the disordered C---Cl bond distances. Similar displacement amplitudes (esd 0.01) were imposed on disordered sites overlapping by less than the sum of van der Waals radii. The site occupancy ratio of the two orientations was allowed to freely refine.

H atom treatment - All H atoms were included as riding idealized contributors with H atom U's assigned as 1.2 times carrier U_{eq} .

The 1 -1 1, 0 -2 1, -3 2 2, 0 0 2, and -1 0 2 reflections were omitted from the final refinement due to being partially obscured by the beam stop in some orientations.

CCDC: 1834877

References:

- (1) Bruker (2016). APEX3. Bruker AXS, Inc., Madison, Wisconsin, USA.
- (2) L. Krause, R. Herbst-Irmer, G. M. Sheldrick and D. Stalke, *J. Appl. Cryst.*, 2015, **48**, 3-10.
- (3) G. M. Sheldrick, *Acta Cryst.*, 2015, **C71**, 3-8.
- (4) W. C. Hamilton and J. A. Ibers (1968). Hydrogen Bonding in Solids. W.A.Benjamin, Inc., New York, New York, USA.
- (5) H. D. Flack, *Acta Cryst.*, 1983, **A39**, 876-881.
- (6) H. D. Flack and G. Bernardinelli, *J. Appl. Cryst.*, 2000, **33**, 1143-1148.
- (7) A. L. Spek, *Acta Cryst.*, 2009, **D65**, 148-155.
- (8) R. Hooft, L. Straver and A. L. Spek, *J. Appl. Cryst.*, 2008, **41**, 96-103.
- (9) Bruker (2014). APEX2. Bruker AXS, Inc., Madison, Wisconsin, USA.
- (10) G. M. Sheldrick, *Acta Cryst.*, 2015, **A71**, 3-8.
- (11) I. A. Guzei, *J. Appl. Crystallogr.*, 2014, **47**, 806-809.
- (12) Bruker (2014). TWINABS. Bruker AXS, Inc., Madison, Wisconsin, USA.
- (13) A. L. Spek and P. van der Sluis, *Acta Cryst.*, 1990, **A46**, 194-201.
- (14) G. M. Sheldrick, (2008). Cell_Now. Program to isolate multiple orientations for crystals suffering from non-merohedral twinning. Institute fur anorg chemie, Göttingen, Germany.
- (15) Bruker (2014). SAINT, SHELXTL, XCIF, XPREP. Bruker AXS, Inc., Madison, Wisconsin, USA.
- (16) Bruker (2014). TWINABS. Bruker AXS, Inc., Madison, Wisconsin, USA.